J Mater Sci (2009) 44:4455–4459
DOI 10.1007/s10853-009-3673-7

Sol–gel combustion synthesis of nanocrystalline $LaMnO_3$ powders and photocatalystic properties

Yuanyuan Li · Shanshan Yao · Lihong Xue · Youwei Yan

Received: 14 January 2009 / Accepted: 8 June 2009 / Published online: 18 June 2009

Abstract A novel $LaMnO_3$ photocatalyst with perovskite structure was prepared by sol–gel combustion method. The combustion reaction mechanisms of nanocrystalline $LaMnO_3$ powders were investigated by thermal analysis, infrared spectra, and X-ray diffraction technique. The results showed that the gels exhibited self-propagating behavior after ignition in air. Nanocrystalline $LaMnO_3$ powders can be synthesized in one step by using sol–gel combustion synthesis. The photocatalytic activity of the $LaMnO_3$ powders were evaluated by degradation of methyl orange (MO) in water under UV light irradiation. The results showed that the $LaMnO_3$ powders exhibit good photocatalytic activities under UV light irradiation. The degradation percentage after 36 h on $LaMnO_3$ powders was about 76%.

Abbreviation
MO Methyl orange

Introduction

In recent years, Lanthanum manganites ($LaMnO_3$) with unique electrical, magnetic, and catalytic properties have attracted increasing interests for their applications in solid oxide fuel cells [1], giant magneto resistance [2] and catalytic combustion [3–5]. $LaMnO_3$ has been conventionally synthesized by solid-state reaction. However, conventional solid-state reaction for preparing $LaMnO_3$ powders requires high temperature and usually produces agglomerated particles, which hinders its application in catalysts. Recently, wet-chemical techniques have been applied to prepare $LaMnO_3$ powders such as co-precipitation [6], polymeric gel [7], hydrothermal treatment [8], and sol–gel synthesis [9]. Among them, co-precipitation is difficult to control all cations to precipitate in the solution at the same time, which results in composition segregation. Sol–gel technique usually uses expensive alkoxides as raw materials. Hydrothermal treatment usually needs long time reaction. Thus, study on a simple and economic way to prepare $LaMnO_3$ powders has become an urgent concern.

Sol–gel combustion synthesis has emerged as an attracting technique for the production of highly pure and crystalline oxide powders [10–14]. This technique is based on the sol–gel process and the subsequent combustion process. An aqueous solution containing the desired metal salts and organic fuel forms the gel through sol–gel process, and then the gel is ignited to combust, giving a voluminous and fluffy product with a large surface area. This technique has the advantages of low synthesis temperature, rapid reaction, and one-step synthesis process.

In the present study, we report on the fabrication of nanocrystalline $LaMnO_3$ powders by the sol–gel combustion method. The combustion reaction mechanism, synthesized process, and photocatalystic property of $LaMnO_3$ powders were investigated. The obtained results further extended the application of $LaMnO_3$ to degradation of organic contaminants in water.

Y. Li · S. Yao · L. Xue (✉) · Y. Yan
State Key Laboratory of Materials Processing and Die and Mould Technology, Huazhong University of Science and Technology, Wuhan 430074, People's Republic of China
e-mail: xuelh@mail.hust.edu.cn

Experimental procedure

Catalyst preparation

Analytical-grade lanthanum nitrate ($La(NO_3)_3 \cdot 6H_2O$), manganese nitrate ($Mn(NO_3)_2 \cdot 6H_2O$), and citric acid ($C_6H_8O_7 \cdot H_2O$) were used as raw materials. According to the principle of propellant chemistry, the net oxidizing valence of the metal nitrate should be equal to the net reducing valence of the fuel for the stoichiometric redox reaction between fuel and oxidant. The reaction between citric acid and metal nitrates for $LaMnO_3$ synthesis is presented as Eq. 1:

$$36La(NO_3)_3 \cdot 6H_2O + 36Mn(NO_3)_2 \cdot 6H_2O + 50C_6H_8O_7 \cdot H_2O \xrightarrow{NH_3 \cdot H_2O} 36LaMnO_3 + 90N_2 \uparrow + 300CO_2 \uparrow + 682H_2O \uparrow \quad (1)$$

Appropriate amount of metal nitrates and citric acid were firstly dissolved in distilled water. The pH value of the mixed solution was adjusted to 7 by addition of ammonia. The obtained transparent solution was then heated at 130 °C for 24 h on a hot plate with continuous stirring for dehydration. During dehydration process, polycondensation reaction happened between citric acid and nitrates, and a transparent gel formed. The gels were put into oven preheated to 300 °C. After a few minutes, the gel was ignited and burnt in a self-propagating combustion manner until all gels were completely burnt out to form oxide product.

Catalyst characterizations

The thermal decomposition behavior of the gels was characterized by thermogravimetric and differential thermal analysis (DTA/TG, STA 409) at a heating rate of 10 °C/min in air. The phase identification of the as-synthesized powders was performed using X-ray diffractometer (XRD, Philips PW 1710) with Cu$K\alpha$ radiation ($\lambda = 1.5405$ Å). The functional groups of the products were detected by infrared spectra (IR, VERTEX 70). The BET surface area of the catalyst samples was calculated from the nitrogen adsorption/desorption isotherms. These isotherms were determined at the liquid nitrogen temperature (77 K) using a Micromeritics ASAP2100 automatic equipment. UV–Vis diffuse reflectance spectrums (DRS) of the samples were measured by using Hitachi U-3010 UV–Vis spectrophotometer. The obtained diffuse reflectance spectra were converted to absorption spectra on the basis of the Kubelka–Munk theory. The morphology of the as-synthesized powders was observed by scanning electron microscopy (SEM, SIRION 200).

Photocatalytic reactions

The photocatalytic activities of nanocrystalline $LaMnO_3$ powders were valued by the decomposition of MO in water. The optical system for the photocatalytic reaction was a 40 W high-voltage mercury lamp with a maximum emission at 360 nm. The photocatalytic reaction procedures were as follows: MO solutions (300 mL, 10 mgL^{-1}) containing 0.6 g of $LaMnO_3$ powders were put in a glass beaker. Prior to irradiation, the suspensions were magnetically stirred without UV irradiation for 30 min to establish adsorption/degradation equilibrium. The distance between the liquid surface and the light source was about 8 cm. During irradiation, 5 mL suspension was successively taken from the reaction cell at given time intervals and separated through centrifugation (4200 rpm, 15 min). The supernate was analyzed by recording variations of the absorption band maximum (464 nm) in the UV–Vis spectra of MO by using a UV–Vis spectrophotometer (Hitachi U-3010).

Results and discussion

DTA/TG results of the xerogel precursor are shown in Fig. 1. It can be seen that there is one slight endothermic peak and one sharp exothermic peak in the DTA curve. The sight endothermic peak appears at around 100 °C accompanied by 5% weight loss in the TG curve are ascribed to loss of residual water in the gel. The sharp exothermic peak, at about 250 °C is nearly vertical in the DTA trace, accompanied by a drastic weight loss at the same temperature is caused by the autocatalytic anionic oxidation–reduction reaction between the nitrates and citric acid. The weight loss associated with this sharp exothermic peak is

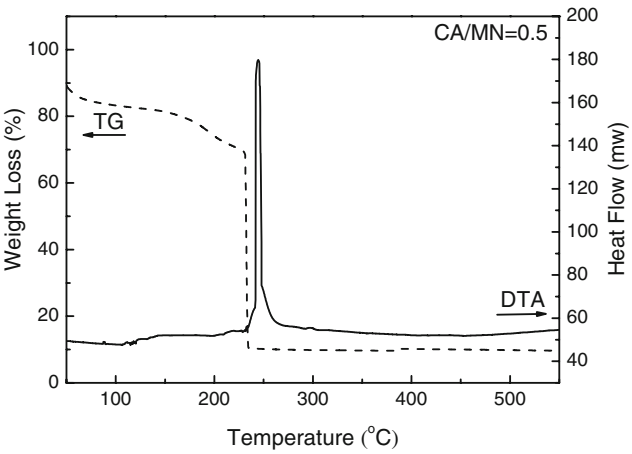

Fig. 1 DTA/TG traces for the xerogel precursor

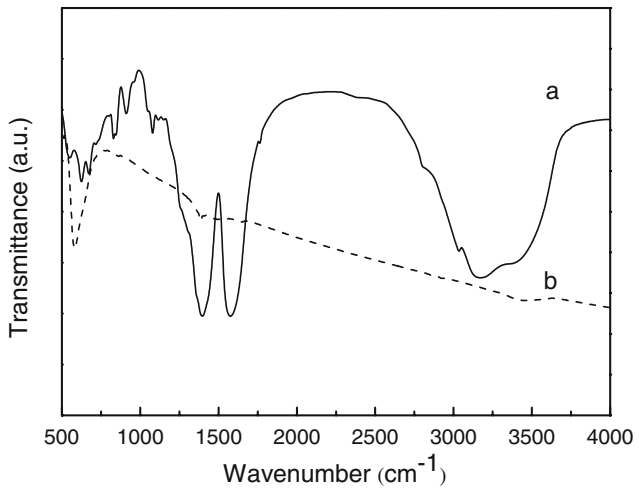

Fig. 2 FT-IR spectra of: (a) the xerogel and (b) the as-synthesized powders

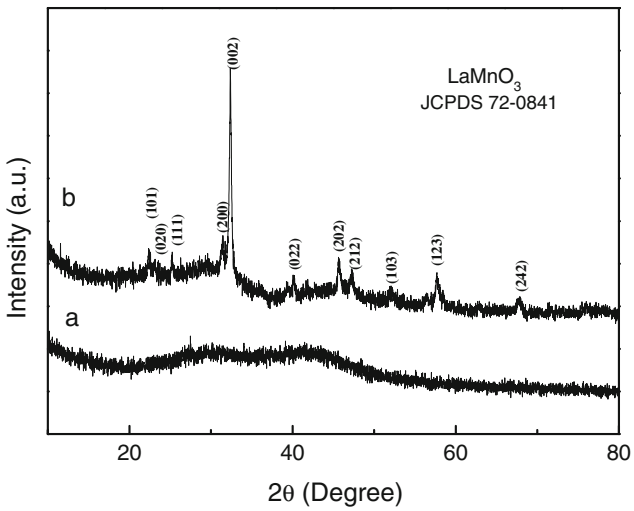

Fig. 3 XRD patterns of: (a) the xerogel and (b) the as-synthesized powders

about 60%, in good agreement with the value calculated from the reaction of Eq. 1.

Figure 2 shows the FT-IR spectra of the dried gels and as-synthesized powders in the range from 500 to 4000 cm^{-1}. The spectra of dried gel (Fig. 2a) shows that the characteristic bands of the O–H stretching vibration in water and citric acid are at about 3200 and 670 cm^{-1} [10, 15], while the anti-symmetrical and symmetrical stretching vibration bands of carboxyl ion related to citric acid are located at 1620 cm^{-1} [16, 17]. The bands located at 1380 and 820 cm^{-1} are ascribed to the N–O bending vibration of NO_3^- [17]. After combustion, the characteristic bands of NO_3^-, O–H, and carboxyl ion almost disappeared (Fig. 2b). On the other hand, it appears a significant spectroscopic band at about 600 cm^{-1} corresponding to the stretching mode involving the internal motion along the length of the Mn–O–Mn or Mn–O bond [18]. The disappearance of the characteristic bands of the carboxyl ion and NO_3^- ions in the FT-IR spectra of as-synthesized powder suggests that carboxyl ions and NO_3^- ions take part in the reaction during combustion. Thus, the combustion can be considered as a thermally induced anionic redox reaction of the gel wherein the carboxyl group act as reductant and NO_3^- ions act as oxidant, as reported by Chakrabarti et al. [19].

XRD analysis was used to aid further interpretation of the reaction processes. Figure 3 shows the XRD patterns of xerogel and as-synthesized powders. The xerogel powder is amorphous in nature. The as-synthesized powder is a single phase $LaMnO_3$ with perovskite structure. This indicates that the $LaMnO_3$ powders can be directly formed after the auto-combustion of the gel without further calcination. The crystalline size of the as-synthesized powder estimated from the half-width of (002) peak via the Scherrer formula:

$$D = \frac{0.9\lambda}{\beta \cos\theta}$$

where D is the crystallite size in nm, λ is the radiation wavelength (0.15405 nm for Cu$K\alpha$), β is the corrected half-width, and θ is the diffraction peak angle. The calculated crystallite sizes are 29.8 nm.

Figure 4 shows the SEM micrographs of the as-synthesized powders. The powder has spongy aspect consisted of agglomerates and large number of pores. The size of the pore was found to be in the range of 0–2 μm. It is well-known that the surface area of a catalyst greatly affects its catalytic activity. The BET measurement showed that the surface area of as-synthesized $LaMnO_3$ powders prepared by sol–gel combustion method was about 33 $m^2\ g^{-1}$.

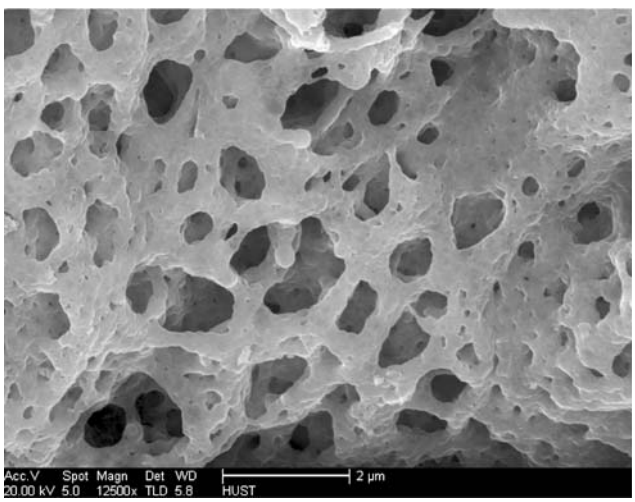

Fig. 4 SEM image of $LaMnO_3$ prepared by sol–gel combustion synthesis

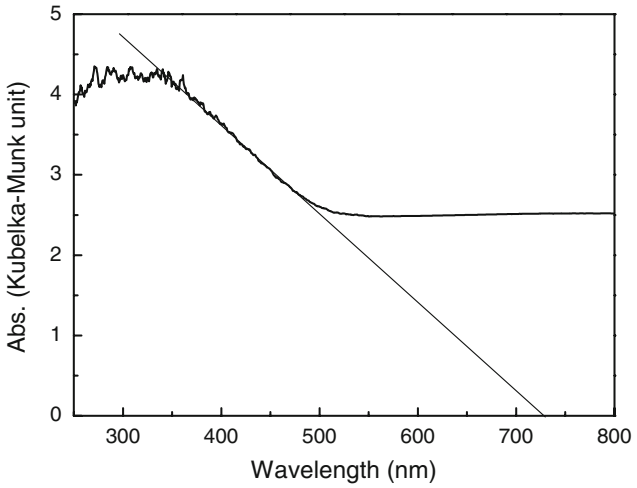

Fig. 5 Kubelka–Munk conversion spectrum of $LaMnO_3$ powders

Figure 5 shows the Kubelka–Munk spectra of $LaMnO_3$ powders. The characteristic absorption edge for $LaMnO_3$ is approximately at about $\lambda = 730$ nm, possessing potential photocatalytic activity. Photocatalytic processes are based on electron/hole pairs generated by band gap radiation, which can give rise to redox reactions with species absorbed on the surface of the catalysts. Therefore, it was considered that the $LaMnO_3$ powders would exhibit photocatalytic properties because of their photoabsorption properties.

MO solution was used to evaluate the photocatalytic activity of the $LaMnO_3$ powders. Figure 6 shows the absorption spectral changes of the MO solution decomposition of the $LaMnO_3$ powders prepared by sol–gel combustion method. Inset of Fig. 6 is the temporal evolution of the concentration (C/C_0) of MO, in which C_0 and C represent the initial equilibrium concentration and reaction concentration of MO, respectively. As it can be seen, the catalyst exhibited good activity in the degradation of MO solution under UV light. The concentration of MB decreased with the increasing of radiation time. The degradation percentage after 36 h on $LaMnO_3$ powders was about 76%. A gradual decrease in the absorption intensity at 464 nm can be observed, indicating that the MO molecule has been degraded. The significant temporal changes in the concentration of the MO clearly proved the photocatalytic activity of $LaMnO_3$ powders under UV light irradiation.

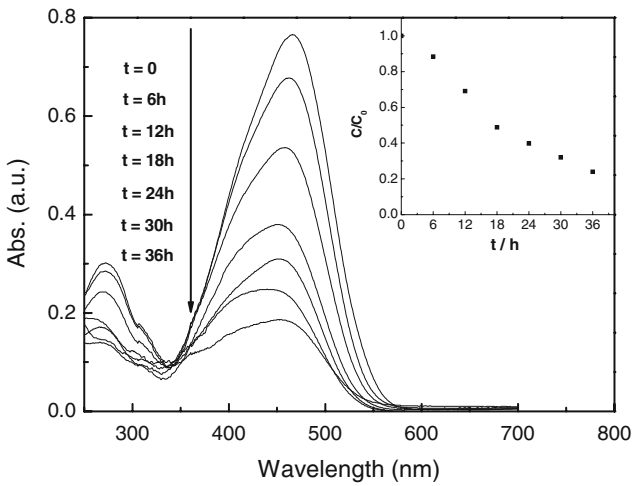

Fig. 6 Photodegradation of MO monitored as the normalized concentration change versus irradiation time under UV light irradiation (insert) and absorption changes of MO solution on $LaMnO_3$ powders

Conclusion

The nanocrystalline $LaMnO_3$ powders can be synthesized by the sol–gel combustion method using corresponding metal nitrates as oxidizers and citric acid as fuel. The combustion can be considered as a thermally induced autocatalytic anionic redox reaction of the gel. After combustion, the gel is directly transformed into a single phase $LaMnO_3$ powders with spongy aspect. The nanocrystalline $LaMnO_3$ powders exhibited a good activity in the degradation of MO under UV light irradiation. The degradation percentage of MO after 36 h on $LaMnO_3$ powders was about 76%, indicating good photocatalytic activity of the obtained $LaMnO_3$ powders.

Acknowledgment This work is financially supported by the National Natural Science Foundation of China, NNSFC 50574042.

References

1. Holtappels P, Bagger C (2002) J Eur Ceram Soc 22:41
2. Nagaev EL (2001) Phys Rep 346:387
3. Giannakis AE, Ladavos AK, Pomonis PJ (2004) Appl Catal B 49:147
4. Spinicci R, Faticanti M, Marini P et al (2003) J Mol Catal A 197:147
5. Cimino S, Pirone R, Lisi L (2002) Appl Catal B 35:243
6. Uskokovic V, Drofenik M (2007) Mater Des 28:667
7. Bell RJ, Millar GJ, Drennan J (2000) Solid State Ionics 131:211
8. Choudhary VR, Banerjee S, Uphade BS (2000) Appl Catal B 197:183
9. Hwang HJ, Awano M (2001) J Eur Ceram Soc 21:2103
10. Mali A, Ataie A (2005) Scr Mater 53:1065
11. Yue ZX, Guo WY, Zhou J et al (2004) J Magn Magn Mater 270:216
12. Liu XJ, Li HL, Xie RJ et al (2007) J Lumin 124:75
13. Xiao Q, Si ZC, Yu ZM et al (2007) Mater Sci Eng B 137:189
14. Sun J, Zhang ZH, Cao XH (2007) Solid State Phenom 121–123:967

15. Predoana L, Malic B, Kosec M et al (2007) J Eur Ceram Soc 27:4407
16. Ponce S, Fierro JLG (2000) Appl Catal B 24:193
17. Choso T, Tabata K (1997) J Solid State Chem 129:60
18. Nagabhushana BM, Chakradhar RPS, Ramesh KP et al (2007) Mater Chem Phys 102:47
19. Chakrabarti N, Maiti HS (1997) Mater Lett 30:169